BOREAL ENVIRONMENT RESEARCH 16: 407–416
ISSN 1239-6095 (print) ISSN 1797-2469 (online)

Helsinki 31 October 2011

Remote sensing based estimates of surface wetness conditions and growing degree days over northern Alberta, Canada

M. Shammi Akther and Quazi K. Hassan*

Department of Geomatics Engineering, Schulich School of Engineering, University of Calgary, 2500 University Dr NW, Calgary, Alberta T2N1N4, Canada (corresponding author's e-mail: qhassan@ucalgary.ca)

Received 18 Oct. 2010, accepted 17 Dec. 2010 (Editor in charge of this article: Hannele Korhonen)

Akther, M. S. & Hassan, Q. K. 2011: Remote sensing based estimates of surface wetness conditions and growing degree days over northern Alberta, Canada. *Boreal Env. Res.* 16: 407–416.

Here, our aims are to estimate two most important climate-driven variables of the surface wetness condition (SWC) and growing degree days (GDD: a temperature regime) primarily using remotely sensed 8-day composites from Moderate-resolution Imaging Spectrometer (MODIS) sensor over the agriculture and forest-dominated regions in the Canadian province of Alberta. The estimation of both SWC and GDD was based on exploiting relations between surface temperature and vegetation indices. Our results showed that on average in 81.67% of the cases, the MODIS-derived SWC values differed less that ±20% from the ground-based measurements of volumetric soil moisture. The MODIS-derived GDD values differed less ±20% from the ground-based measurements of GDDs in 90.39% of the cases.

Introduction

It is well recognized that climate-driven variables are critical for both agriculture and forestry (Cosh *et al*. 2010, Latta *et al*. 2009, Palm *et al*. 2010). Two most important such variables are the surface wetness condition (SWC, indirectly indicating soil moisture (SM), i.e. the amount of water in the soil column available to plants); and growing degree days (GDD). These variables are crucial for vegetation growth and many plant functions (e.g., photosynthesis, transpiration, both plant and soil respiration, water and nutrient movements within plant, etc.) (Flanagan and Johnson 2005, Hari and Nöjd 2009). They both can be measured precisely *in situ* using various methods. However, the ground-based methods fail to provide the spatial variability, which is important for understanding the dynamics at the landscape scale. One of the feasible alternatives are remote sensing methods, which have already been proven to address the spatial dynamics for the variables of interest (Anttila and Kairesalo 2010, Sekhon *et al*. 2010, Stenberg *et al*. 2008).

For the last two decades, visible and thermal infrared remote-sensing data were widely used to determine SWC. In most cases, SWC can be derived from the relationships between the vegetation index (VI) and the actual surface temperature (T_s) (Carlson 2007, Li *et al*. 2009, Patel *et al*. 2009). A two dimensional scatter plot of T_s-VI usually assumes a triangular (Sandholt *et al*. 2002, Carlson 2007) or a trapezoidal shape (Moran *et al*. 2004, Petropoulos *et al*. 2009). The

edges of these shapes are considered in estimating SWC (*see* section *Estimation of TVWI* below for more details). In general, the negative slope of the T_s-VI diagram describes the water availability with respect to the vegetation conditions, e.g., (i) high SWC values are found for relatively dense vegetation with low T_s values; and (ii) low SWC values are found for sparse vegetation with high T_s values. To describe the VI component, the normalized difference vegetation index (NDVI: as a function of surface-reflectance values from red and near-infrared spectra; Parviainen *et al*. 2010) is used. The T_s-VI space can be defined by using either daily or composite values. However, Venturini *et al*. (2004) emphasized uncertainty of the daily T_s values acquired by means of remote sensing resulting from atmospheric conditions. They also mentioned that the use of a multiday (e.g., 14- or 16-day) composite of T_s would not be useful for their proposed method of determining ϕ (i.e., the combined effects of Prestley-Taylor's α and Budyko-Thronwaite-Mather's wetness parameters) as a part of estimating evapotranspiration by using the T_s-VI relation. Other researchers (e.g., Patel *et al*. 2010, Chen *et al*. 2010) used composites in the T_s-VI approach for determining SWC regimes, and demonstrated their effectiveness.

Despite the wider acceptability of the T_s-VI method, the major limitation is its applicability over a topographically variable terrain (Carlson 2007), and the fact that it has not been widely used over vegetated regions. The topographic-variability limitation was first addressed by Hassan *et al*. (2007b) for the forest-dominated humid region in the Canadian Atlantic Maritime Ecozone. It was done by transforming T_s into a potential surface temperature (θ_s), i.e. T_s with removed effect of elevation by recalculating the temperateure at the site for the mean sea level, and then combining it with NDVI (the method described as the temperature-vegetation-wetness index, TVWI) (Hassan *et al*. 2007b, Hassan and Bourque 2009). However, the TVWI approach requires further validation over other ecozones to determine its wider applicability.

On the other hand, several studies demonstrated that remote sensing data were also effective in calculating GDD as a function of remote-sensing based T_s (Hassan *et al*. 2007a, 2007c, Neteler 2010). In Hassan *et al*. (2007a, 2007c), the initial step was to convert the MODIS-based 8-day composites of T_s (acquired between 10:30 and 12:00) into 8-day mean values using an empirical relationship. This relationship was built by using ground-based emitted longwave radiation data (by way of applying Stefan-Boltzman's equation; Langer *et al*. 2010). In reality, such longwave radiation data might be difficult to avail in other places. Thus, we propose to convert the MODIS-based T_s by establishing an empirical relation between T_s and the ground-based air temperature (T_a) measured at the meteorological stations within the area of interest. In theory, the availability of such meteorological stations is relatively better across the globe (the networks of Ameriflux, fluxnet-Canada, CarboEurope, Chinaflux, etc.).

In this paper, we aim: (i) to implement the TVWI approach over the topographically-variable agriculture and forest-dominated northern portion of the Canadian province of Alberta, and to assess its ability of capturing the ground-based measured volumetric soil moisture (VSM); (ii) to calculate GDDs over the growing season (i.e., April–October) by integrating MODIS-based T_s and ground-based T_a, and evaluating the modeled GDD by comparing it with the ground-based measured GDD.

Study area and data requirements

The extent of the study area is geographically between 53°–60°N and 108°–120°W (Fig. 1). It falls into the northern portion of the Canadian province of Alberta. It can be characterized as topographically variable (i.e., average elevation varies from 225 m to 1750 m a.s.l.) with the dominance of agriculture and forest land-cover types (*see* Fig. 1 for more details). The average annual temperature across the study area varies between –3.6 and +2.3 °C; the mean annual precipitation varies between 300–900 mm (Dowing and Pettapiece 2006).

In this study, we primarily used Moderate Resolution Imaging Spectroradiometer (MODIS based products freely available from the Land Processes Distributed Active Archive Center (LP DAAC: a component of NASA's earth observing

system data and information system) (https://lpdaac.usgs.gov/lpdaac/products/modis_products_table). Those included: (i) MOD11A2 ver. 005: 8-day composites of T_s (generated by averaging the clear-sky daytime T_s values over 8-day periods) at 1-km resolution in April–October 2005–2008; (ii) MOD09Q1 ver. 005: 8-day composites of red (620–670 nm) and near-infrared (NIR: 841–876 nm) surface reflectance at 250 m resolution in May–September 2006–2008; (iii) MOD13Q1 ver. 005: 16-day composite of EVI (enchanced vegetation index) at 250-m resolution during April–October 2005–2008. We also used a digital elevation model (DEM) of the study area at 250-m resolution generated from 3-arc-second resolution height point-data freely available from the NASA Shuttle Radar Topography Mission archive (http://srtm.csi.cgiar.org). In addition, we used ground-based measurements of daily mean: (i) T_a from 77 stations, freely available from Environment Canada (http://climate.weatheroffice.ec.gc.ca); (ii) VSM from 13 stations (5-cm, 20-cm, 50-cm and 100-cm depths acquired using Theta-Probe-type ML2x), freely available from Alberta Agriculture and Rural Development Department (http://www.agric.gov.ab.ca/app116/stationview.jsp) for the same period as the remote sensing data; and (iii) long-term (i.e., 1971–2000) average GDD data from 52 stations, freely available from Environment Canada (http://climate.weatheroffice.ec.gc.ca).

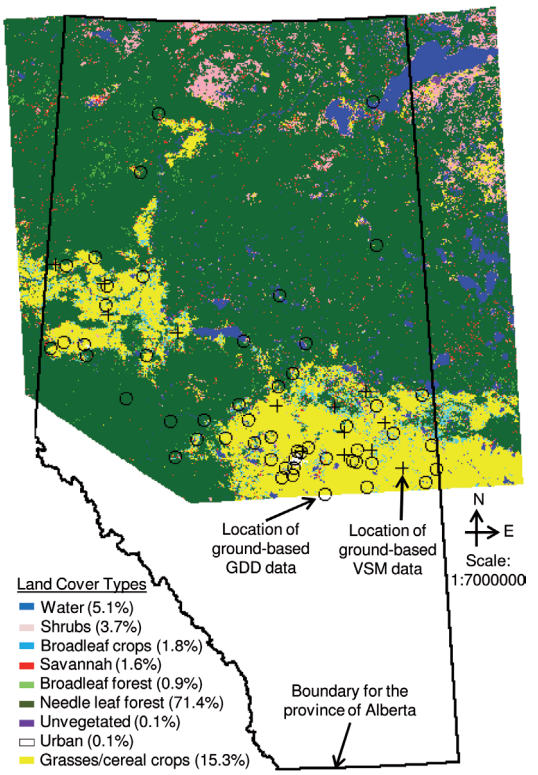

Fig. 1. The study area (53°–60°N, 108°–120°W) with a land-cover map derived from annual composite of 2004 MODIS images (i.e., MOD12Q1 ver. 004; annual 1-km composite of 2004 MODIS images). Crosses and circles indicate the locations where the ground-based soil moisture data and GDD data were acquired, respectively.

Methodology

The schematic diagram of the methodology (Fig. 2) has four major components: (i) data pre-processing, (ii) estimating TVWI values, (iii) generating GDD values, and (iv) comparing the TVWI and GDD values with respective ground-based measurements.

Data pre-processing

The acquired raw MODIS-based surface reflectance, T_s and EVI were originally provided in sinusoidal projection. We used a MODIS Reprojection Tool ver. 4.0 (freely available at https://lpdaac.usgs.gov/lpdaac/tools/modis_reprojection_tool) to reproject the images into UTM Zone 12 NAD 83. Two contiguous images were mosaicked to achieve the desire study area, and again reprojected into Ten Degree Transverse Mercator (10TM) NAD 83 (a widely used projection system by the Alberta Government) as Zone 12 of the UTM projection was unable to span over the entire study area. Among the MODIS-based products, the surface reflectance images (MOD09Q1) were used to calculate NDVIs. We observed cloud contamination in both NDVI and T_s images. In order to correct this, we adopted an image correction technique developed by Hassan *et al.* (2007a, 2007b), which was used to fill the cloud-contaminated pixels in the NDVI and T_s time series. The formulas are:

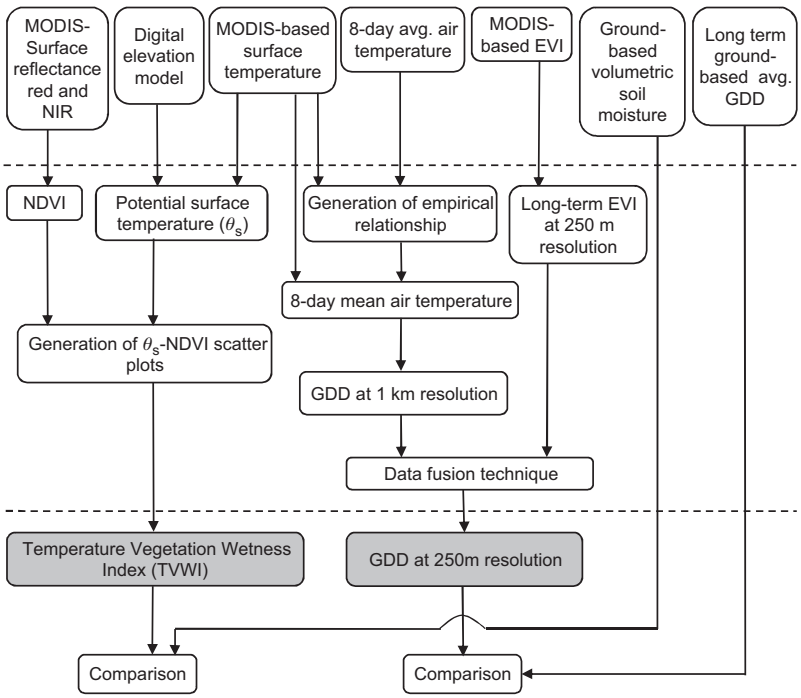

Fig. 2. Diagram of the methodology.

$$A = \frac{\sum_{i=1}^{n} \overline{x}_i - x_i}{m}, \text{ and} \quad (1)$$

$$B = \overline{x}_i - A, \quad (2)$$

where A is the average deviation of either T_s or NDVI from their respective $\overline{x}_i$'s for a specific cloud-contaminated pixel of interest, $\overline{x}_i$ is the 8-day composite mean value of either T_s or NDVI for a specific year for the entire image, i is the 8-day period of interest, and n is the total number of 8-day composite images in a year; x_i the image-based T_s or NDVI value from cloud-free 8-day composites, m is the total number of cloud-free pixels from individual composite images available for a specific year for a cloud-contaminated pixel, and B is the estimated 8-day mean of either T_s or NDVI for an individual cloud-contaminated pixel.

Estimation of TVWI

The estimation of TVWI was performed in two steps proposed by Hassan *et al*. (2007b): (i) converting the T_s into θ_s; and (ii) interpreting the observed scatter plots of θ_s–NDVI.

To convert T_s into θ_s, the following expressions were used (Hassan *et al*. 2007b, Hassan and Bourque 2009):

$$p = 101.3 \left[\frac{293 - 0.0065z}{293} \right]^{5.26}, \quad (3)$$

$$\theta_s = T_s \left(\frac{p_o}{p} \right)^{\frac{R}{C_p}}, \quad (4)$$

where p is the atmospheric pressure (kPa), z is the elevation above the mean sea level (m), T_s is the actual surface temperature (K); p_o is the average pressure at the mean sea level (= 101.3 kPa), R is the gas constant (= 287 J kg^{-1} K^{-1}), C_p is the specific heat capacity of air (~1004 J kg^{-1} K^{-1}), and θ_s is the potential surface temperature (K).

In general, we received trapezoidal shapes upon generating the scatter plots of θ_s–NDVI for each of the 8-day periods (*see* Fig. 3). Both the dry (i.e., θ_{dry}, K) and wet (i.e., θ_{wet}, K) edges describe available water conditions in relation to vegetation conditions. Along θ_{dry}, water for evapotranspiration is most likely unavailable, thus the values of TVWI would equal 0, and along

θ_{wet}, water for evapotranspiration is unrestricted, thus the values of TVWI would equal 1.

Finally, TVWI is calculated using the following expression (Hassan *et al*. 2007b, Hassan and Bourque 2009):

$$\mathrm{TVWI} = \frac{\theta_{dry} - \theta_s}{\theta_{dry} - \theta_{wet}}, \quad (5)$$

Generation of GDD

In generating GDD maps, the following steps were carried out: (i) converting the MODIS-based instantaneous 8-day composites of T_s into the equivalent 8-day mean T_a, and calculating the GDD values at 1-km resolution; and (ii) enhancing the spatial resolution of the GDD map from 1 km to 250 m, so that it would be consistent with the spatial resolution of the TVWI maps.

The daily mean T_a values from 77 meteorological stations (*see* Fig. 1 for location information) were transformed into 8-day means for the same 8-day periods as the MODIS data. For those stations, we also extracted the MODIS-based instantaneous 8-day composites of T_s. Then, using Microsoft Excel 2007, we performed a linear-regression analysis for these two variables (*see* Fig. 4a). It revealed that a reasonably strong relation existed ($r^2 \approx 0.68$, slope = 0.59 ± 0.01, intercept = 111.73 ± 3.09 at 95% confidence level for the regression line, $p < 0.0001$) during the period 2005–2007. In order to evaluate how the function given in Fig. 4a can predict the 8-day mean T_a, we used this relation to calculate T_a using 8-day MODIS-based T_s for 2008. The analysis revealed that also this relationship was reasonabley strong ($r^2 \approx 0.67$, slope = 0.65 ± 0.021, intercept = 99.71 ± 5.83 at 95% confidence level for the regression line, $p < 0.0001$) between the measured and predicted values (*see* Fig. 4b). Both phases (calibration and validation, *see* Fig. 4) demonstrated similar levels of agreement (i.e., $r^2 \approx 0.67$), and the discrepancies (≈33% of the cases) were due to the fact that the T_a values were acquired at point locations but the MODIS-based T_s values were averages for 1×1 km^2 areas.

Considering the above, using the function given in Fig. 4a, we calculated equivalent 8-day mean T_a values. We then used these values in the following expression to calculate seasonally accumulated GDDs:

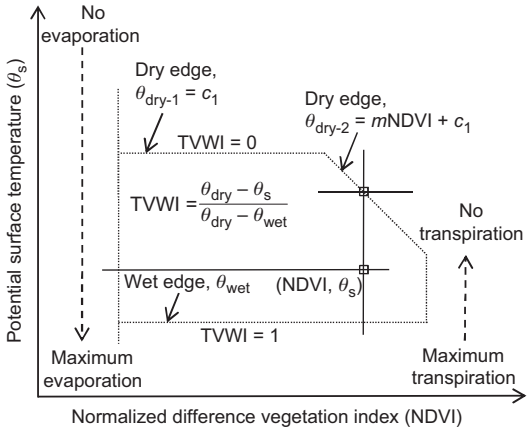

Fig. 3. Conceptual diagram illustrated the calculations of TVWI as a function of θ_s and NDVI. Both of the dry edge (i.e., θ_{dry}) and wet edge (i.e., θ_{wet}) would describe the available water conditions in relation to vegetation conditions. c_1 is the dry edge for θ_{dry1}; m and c_2 are the slope and intercept for θ_{dry2}, respectively. Modified after Hassan *et al*. 2007b.

$$\mathrm{GDD} = \sum_{i=1}^{n} \left(\bar{T}_{ai} - T_{base} \right), \quad (6)$$

where T_{base} equals 5 °C (= 278.15 K), and i and n are the first and the last 8-day period of the growing season, respectively, for which the 8-day mean T_a values were calculated.

As the initial spatial resolution of the T_s data was 1 km, the generated GDDs would also be at the same resolution. In order to enhance their spatial resolution, we used the EVI images at the 250-m resolution for data fusion as described in Hassan *et al*. (2007c). Such fusion was possible as the variables of EVI and GDD were found to be ecologically-related (Hassan *et al*. 2007a). With this method, an artificial image (AI) was generated for a 3×3 moving window:

$$\mathrm{AI} = \frac{\mathrm{EVI}_{ins}}{\mathrm{EVI}_{mean}} \quad (7)$$

where EVI_{ins} is the instantaneous value of EVI in the center of the moving window, and EVI_{mean} is the mean of all the EVI values within the moving window. In theory, AI is an index that explains the relation of an instantaneous value of EVI to the mean value of EVI within a given window. It

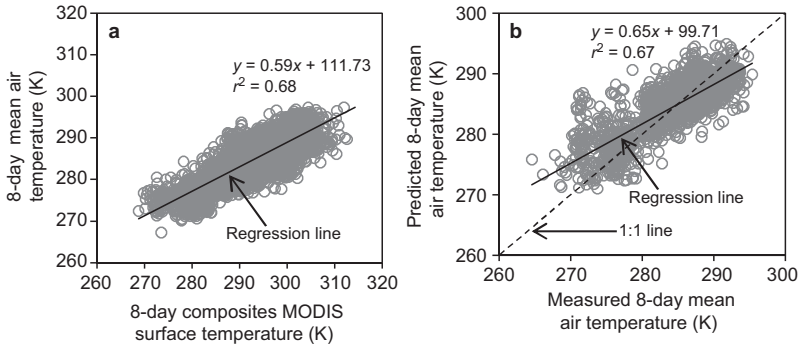

Fig. 4. (**a**) Relation between 8-day composites of the MODIS-based surface temperature (acquired between 10:30 and 12:00 local time) and the ground-based 8-day mean air temperature during 2005–2007 (n = 5691, F = 11987.65, $p < 0.0001$); (**b**) validation of the relation for 2005–2007 and its comparison with the 8-day mean air temperature during 2008 (n = 1874, F = 3857.33, $p < 0.0001$).

also would act as a weight in the calculation of GDD at 250-m resolution:

$$\mathrm{GDD}_{250\mathrm{m}} = \mathrm{AI} \times \mathrm{GDD}_{1\mathrm{km}}, \qquad (8)$$

Validation schema

In this study, we generated a total of 60 TVWI images (i.e., for each 8-day interval) for 2006–2008. At 13 stations (where the ground-based VSM data were acquired; *see* Fig. 1 for location information), we extracted the TVWI values. Then, we calculated an average TVWI value for each of the 8-day intervals. In a similar way, we averaged the ground-based measurement of VSM for each 8-day period of interest. Finally, we compared VSM values with the TVWI values both qualitatively and quantitatively (i.e., "percentage of deviation").

In the case of GDD map, we calculated four seasonal cumulative GDD maps for the period 2005–2008; and then generated an average seasonal cumulative GDD map for the same period. In evaluating such an average seasonal cumulative GDD map, we verified it against the long-term average (i.e., for the period 1971–2000) seasonal ground-based cumulative GDD values from 52 meteorological stations (i.e., the subset of the 77 stations, where the ground-based T_a values were acquired) across the study area. In this case, we also verified how well the average seasonal cumulative GDD values generated with MODIS for 2005–2008 compared to ground measurements from 1971–2000 by calculating a percentage of deviation.

Results and discussion

An example scatter plot of θ_s–NDVI for the days of year (DOY) 153–160 in 2006 is shown in Fig. 5. The value of θ_{dry1} was 318 K, and the slope and intercept of θ_{dry2} were –0.0035 and 344.25, respectively. As in Hassan *et al*. (2007b), the value of θ_{wet} was set at 275 K to establish the same baseline for determining the maximum values of TVWI (= 1) across the whole data series; also at 275 K seems to be sufficient to support evapotranspiration.

An analysis revealed that during 2006–2008 TVWI were in better agreement with VSMs at the 50-cm and 100-cm depths rather than with that at 5 cm or 20 cm (*see* Fig. 6). Similar was also reported by e.g., Su *et al*. (2003). This phenomenon could be explained by the effect of high evapotranspiration on SM at deeper layers. The available SM in the upper soil layers (i.e., at 5–20 cm) would quickly be depleted due to higher evapotranspiration, which would then be supported by the upward movement of SM from deeper layers (≥ 50 cm) (Shuttleworth 1988, Lawrence *et*. *al* 2007). We further performed quantitative evaluation of TVWI and VSM for the 50-cm depth during 2006–2008 (*see* Fig. 7). It revealed that the deviation was

within ±20% in 80% of the cases in 2006, in 65% of the cases in 2007, and in all (100%) cases in 2008. On an average, in 81.67% of the cases, we observed the deviation within ±20% for the period of interest. Besides, relatively higher deviation (i.e., > ±20%) also could be expected as the ground-based measurements were at a point location, while remote sensing-based estimates were an average values over 250 × 250 m^2. In another study (Hassan *et al*. 2007b), the temporal trend lines of the TVWI and VSM values were also found to be significantly related over a humid, forest-dominated region of eastern Canada. For example, the *y* intercepts of TVWI and VSM were on average 32.26% and 33.2%, respectively, during 2003–2005; with all slopes fairly close to 0. It was also demonstrated that the TVWI was strongly correlated with model-derived SM (expressed in % of saturation) with $r^2 = 0.95$.

We also evaluated the deviation between the long-term (1971–2000) average ground-based and MODIS-based average (during 2005–2008) GDD values from 52 stations (*see* Fig. 8). We observed that in 90.39% of the cases, the deviations were within ±20%. In addition to the mentioned earlier reasons for discrepancies, the relatively smaller discrepancies (i.e., > ±20% in ~9.61% of the cases) between the two GDD datasets were also due to the representative periods (i.e., 2005–2008 for MODIS data, and 1971–2000 for ground-based measurements). Similar agreements were also found by Hassan *et al*. (2007a), who demonstrated that when considering the MODIS-derived GDD values for

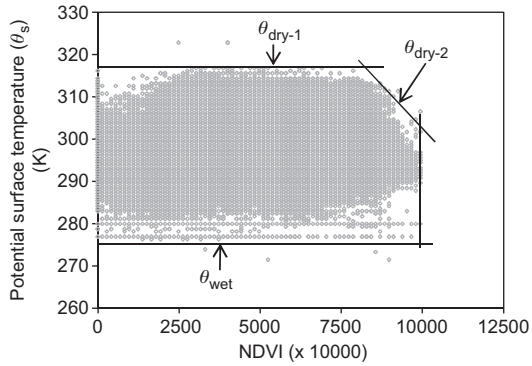

Fig. 5. Example of scatter plot of θ_s–NDVI and the corresponding dry and wet edges during the days 153–160 of the year 2006.

2003–2005, at least 75% of the area within the ecoregion of the interest fell within the reported ranges of GDD values during 1951–1980 over the eastern Canadian province of New Brunswick.

We produced the spatial distribution map of the averaged TVWI and GDD along with their respective relative frequency distributions (*see* Fig. 9). We found that in ~98.81% of the cases the TVWI values fell in the range of 0.2–0.6; with an average and standard deviation of ~0.44 and ~0.083, respectively (*see* Fig. 9a). On the other hand, we found that in ~94.89% of the cases the GDD values fell in the range of 600–1500; with an average and standard deviation of ~977 and ~250, respectively (*see* Fig. 9b). The distinct spatial patterns of both TVWI and GDD are summarized as follows:

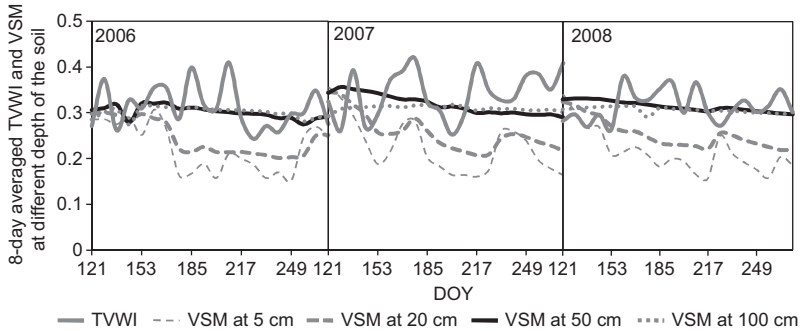

Fig. 6. Temporal dynamics of 8-day averaged TVWI and VSM at different soil depths during the days 121–273 of the years 2006–2008.

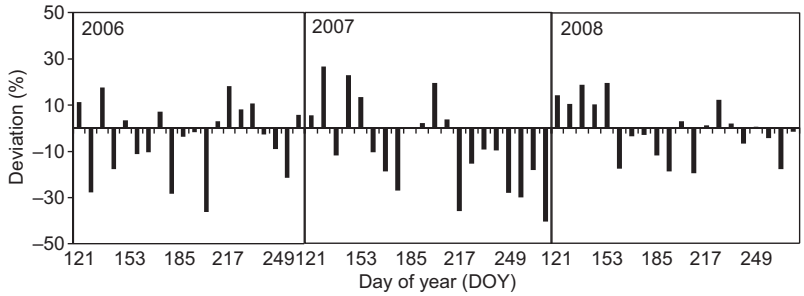

Fig. 7. Deviation between the averaged ground-based measurements of VSM and TVWI for the period 2006–2008.

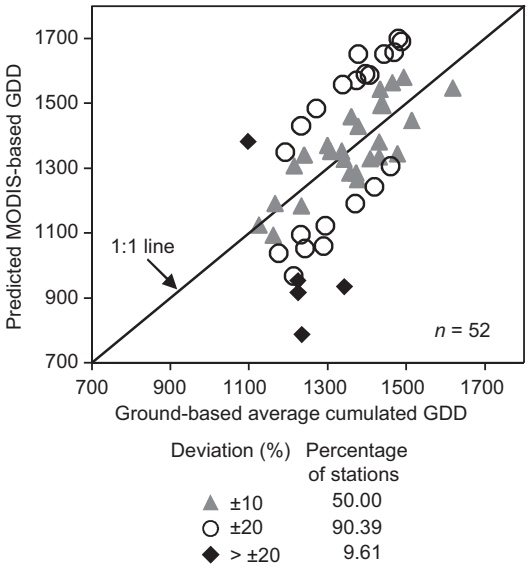

Fig. 8. Comparison between the long-term (1971–2000) average ground-based and MODIS-based average (during 2005–2008) GDD values from 52 stations.

- The higher TVWI values were found in the northern part of the study area, which might be associated with the lower GDD regimes.
- The GDD values were found to be decreasing towards the north which is associated with the gradual decrease in temperature in the same direction.
- In general, the lower TVWI values were mainly observed over agriculture-dominant areas, whereas the higher TWVI values were observed over forest-dominant regions. It might be related to the fact that dense vegetation is able to retain water in the ground better than relatively less vegetated areas.
- We also found that higher GDD values coincided in the same area with relatively lower TVWI values and vice versa. These, in particular, indicate that vegetation plays a key role in regulating its surrounding climatic regimes.
- The TVWI method may be applicable in other ecosystems for assessing VSM conditions over topographically variable forest-dominated regions.
- The GDD method may be efficient in capturing GDDs in different ecosystem, however, calibration of the remote sensing data is necessary.

Concluding remarks

In this paper, we demonstrated the effectiveness of the TVWI approach in capturing the spatial dynamics of surface wetness conditions over agriculture and forest-dominant regions. We found that it could be used as an indirect way of determining soil moisture, because the deviation between the TVWI values and ground-based VSM were found to be within ±20% in 81.67% of the cases. In terms of GDD, we also demonstrated that our method (i.e., integration of MODIS-based T_s and ground-based T_a) was able to depict the spatial variability. We found that the relations between the MODIS-predicted and ground-based GDD values were also reasonably strong (i.e., within ±20% in 90.33% of the cases). Hence, it seems that remote-sensing techniques are suitable for determining these variables over other areas.

Acknowledgments: The authors would like to acknowledge partial funding support from University of Calgary to Dr. Q. Hassan. We also would like to thank the following agencies:

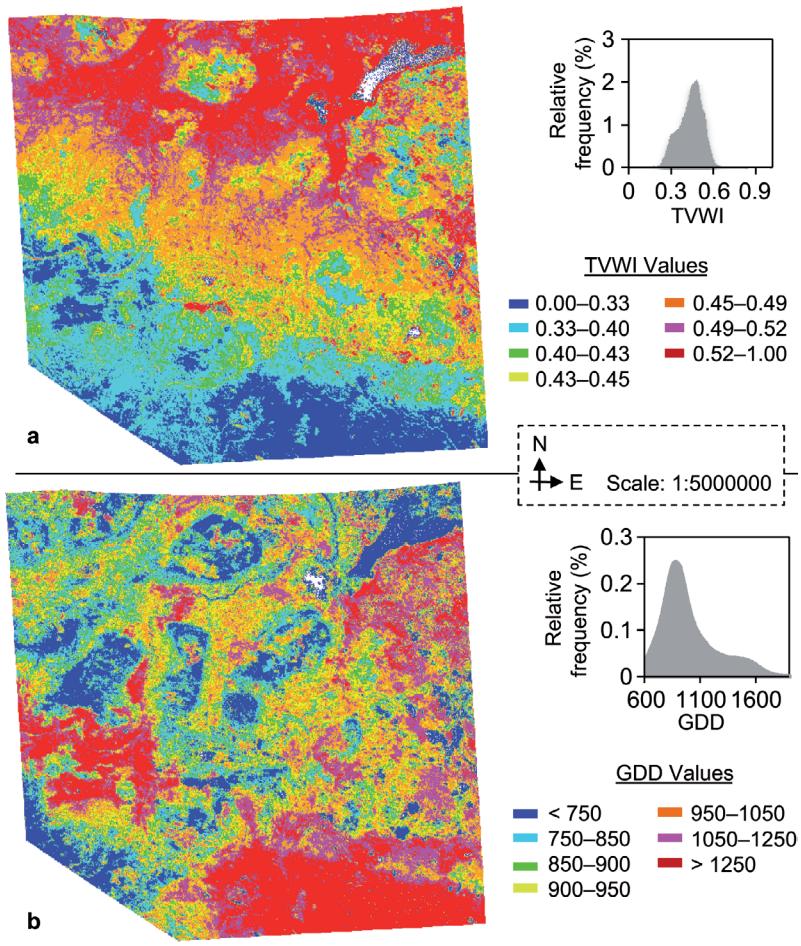

Fig. 9. Spatial dynamics of (**a**) 2006–2008 averaged TVWI and its relative frequency distribution; and (**b**) 2005–2008 averaged GDD and its relative frequency distribution.

(i) NASA for providing MODIS data; (ii) Alberta Agriculture and Rural Development Department for providing ground-based volumetric soil moisture data; and (iii) Environment Canada for providing ground-based mean air temperature and average accumulated GDD data. We also appreciate the comments from the three anonymous reviews on this manuscripts and the editor of this article.

References

Anttila S. & Kairesalo T. 2010. Mean and variance estimations with different pixel sizes: case study in a small water quality monitoring area in southern Finland. *Boreal Env. Res.* 15: 335–346.

Carlson T. 2007. An overview of the "Triangle Method" for estimating surface evapotranspiration and soil moisture from satellite imagery. *Sensors* 7: 1612–1629.

Chen C.F., Son N.T., Chang L.Y. & Chen C.C. 2010. Monitoring of soil moisture variability in relation to rice cropping systems in the Vietnamese Mekong Delta using MODIS data. *Appl. Geography* 31: 463–475.

Cosh M.H., Tao J., Jackson T.J., McKee L.G. & O'Neill P. 2010. Vegetation water content mapping in a diverse agricultural landscape: The National Airborne Field Experiment 2006. *J. Appl. Remote Sens.* 4, 043532, doi: 10.1117/12.871125.

Dowing D.J. & Pettapiece W.W. (eds.) 2006. *Natural regions and subregions of Alberta*. Publication T/852, Natural Regions Committee, Government of Alberta, Alberta, Canada.

Flanagan L.B. & Johnson B.G. 2005. Interacting effects of temperature, soil moisture and plant biomass production on ecosystem respiration in a northern temperate grassland. *Agric. For. Meteorol.* 130: 237–253.

Hari P. & Nöjd P. 2009. The effect of temperature and PAR on the annual photosynthetic production of Scots pine in northern Finland during 1906–2002. *Boreal Env. Res.* 14 (suppl. A): 5–18.

Hassan Q.K. & Bourque C.P.-A. 2009. Potential species distribution of balsam fir based on the integration of biophysical variables derived with remote sensing and process-based methods. *Remote Sens.* 1: 393–407.

Hassan Q.K., Bourque C.P.-A., Meng F.-R. & Richards W. 2007a. Spatial mapping of growing degree days: an application of MODIS-based surface temperatures and enhanced vegetation index. *J. Appl. Remote Sens.* 1, 013511, doi:10.1117/1.2740040.

Hassan Q.K., Bourque C.P.-A., Meng F.-R. & Cox R.M. 2007b. A wetness index using terrain-corrected surface temperature and normalized difference vegetation index derived from standard MODIS products: an evaluation of its use in a humid forest-dominated region of eastern Canada. *Sensors* 7: 2028–2048.

Hassan Q.K., Bourque C.P.-A. & Meng F.-R. 2007c. Application of Landsat-7 ETM+ and MODIS products in mapping seasonal accumulation of growing degree days at an enhanced resolution. *J. Appl. Remote Sens.* 1, 013539, doi: 10.1117/12.782117.

Langer M., Westermann S. & Boike J. 2010. Spatial and temporal variations of summer surface temperatures of wet polygonal tundra in Siberia — implications for MODIS LST based permafrost monitoring. *Remote Sens. Environ.* 114: 2059–2069.

Latta G., Temesgen H. & Barrett T.M. 2009. Mapping and imputing potential productivity of Pacific Northwest forests using climate variables. *Can. J. Forest Res.* 39: 1197–1207.

Lawrence D.M., Thornton P.E., Oleson K.W. & Bonan G.B. 2007. The partitioning of evapotranspiration into transpiration, soil evaporation, and canopy evaporation in a GCM: impacts on land–atmosphere interaction. *J. Hydrometrology* 8: 862–880.

Li Z.L., Tang R., Wan Z., Bi Y., Zhou C., Tang B., Yan G. & Zhang X. 2009. A review of current methodologies for regional evapotranspiration estimation from remotely sensed data. *Sensors* 9: 3801–3853.

Moran M.S., Watts J.M., Peters-Lidard C.D. & McElroy S.A. 2004. Estimating soil moisture at the watershed scale with satellite-based radar and land surface models. *Can. J. Remote Sens.* 30: 805–826.

Neteler M. 2010. Estimating daily land surface temperatures in mountainous environments by reconstructed MODIS LST data. *Remote Sens.* 2: 333–351.

Palm C.A., Smukler S.M., Sullivan C.C., Mutuo P.K., Nyadzi G.I. & Walsh M.G. 2010. Identifying potential synergies and trade-offs for meeting food security and climate change objectives in sub-Saharan Africa. *PNAS* 107: 19661–19666.

Parviainen M., Luoto M. & Heikkinen R.K. 2010. NDVI-based productivity and heterogeneity as indicators of plant-species richness in boreal landscapes. *Boreal Env. Res.* 15: 301–318.

Patel N.R., Anapashsha R., Kumar S., Saha S.K. & Dadhwal V.K. 2009. Assessing potential of MODIS derived temperature/vegetation condition index (TVDI) to infer soil moisture status. *Int. J. Remote Sens.* 30: 23–39.

Petropoulos G., Carlson T.N. & Wooster M.J. & Islam S. 2009. A review of T_s/VI remote sensing based methods for the retrieval of land surface energy fluxes and soil surface moisture. *Prog. Phys. Geography* 33: 1–27.

Sandholt I., Rasmussen K. & Andersen J. 2002. A simple interpretation of the surface temperature/vegetation index space for assessment of surface moisture status. *Remote Sens. Environ.* 79: 213–224.

Sekhon N.S., Hassan Q.K. & Sleep R.W. 2010. Evaluating potential of MODIS-based indices in determining "snow gone" stage over forest-dominant regions. *Remote Sens.* 2: 1348–1363.

Shuttleworth W.J. 1988. Evaporation from Amazonian rainforest. *Proc. Roy. Soc. London B* 233: 321–346.

Stenberg P., Rautiainen M., Manninen T., Voipio P. & Mottus M. 2008. Boreal forest leaf area index from optical satellite images: model simulations and empirical analyses using data from central Finland. *Boreal Env. Res.* 13: 433–443.

Su Z., Yacob A., Wen J., Roerink G., He Y., Gao B., Boogaard H. & Diepen C.V. 2003. Assessing relative soil moisture with remote sensing data: theory, experimental validation, and application to drought monitoring over the North China Plain. *Phys. Chem. Earth* 28: 89–101.

Venturini V., Bisht G., Islam S. & Jiang L. 2004. Comparison of evaporative fractions estimated from AVHRR and MODIS sensors over south Florida. *Remote Sens. Environ.* 93: 77–86.